Proceedings World Geothermal Congress 2010
Bali, Indonesia, 25-29 April 2010

Hydrothermal System Beneath Usu Volcano Inferred from Self-potential Observation and Numerical Simulation

Hideaki Hase[1], Tekeshi Hashimoto[2], Yasunori Nishida[3], Mitsuru Utsugi[4], Hiroyuki Inoue[5], and Mizue Saba[6]

[1]Earthquake Research Institute, Tokyo University, 1-1-1 Yayoi, Bunkyo-ku, Tokyo 113-0032, Japan

[1, 2, 3]Institute of Seismology and Volcanology, Hokkaido University, West8, North10, Kita-ku, Sapporo 060-0810, Japan

[4, 5]Institute for Geothermal Science, Graduate School of Science, Kyoto University, Minami-Aso, Aso, Kumamoto 869-1404, Japan

[6]Geothermal Energy Research & Development Co., Ltd., Shinkawa 1-22-4, Chuo, Tokyo 104-0033, Japan

hase@eri.u-tokyo.ac.jp

Keywords: hydrothermal system, self-potential, Usu volcano

ABSTRACT

Usu volcano is located at southwestern part of Hokkaido, which is one of the most active volcanoes in Japan. We conducted self-potential (SP) surveys on the volcano, since July to December 2006. The compiled SP map reveals positive anomalies around Gin-numa crater and northwestern part of Ko-Usu, and a negative anomaly on the top of O-Usu lava dome on the summit caldera. The locations of the positive anomalies are corresponding to the fumarolric area, which are likely to be affected by hydrothermal system beneath the volcano. To confirm the consideration, we conducted numerical simulations of groundwater flow and SP of the electrokinetic origin within the volcano. The simulation results indicated the existences of, (a) hydrothermal upwelling driven by the intruded conduit beneath Usu-shinzan as a heat source, (b) a caprock layer at the upper margin of the hydrothermal and (c) low-resistivity channels from the upper margin of the hydrothermal area to the surface.

1. INTRODUCTION

Self-potential (SP) surveys have been carried out at many active volcanoes and observed positive anomalies over several hundred mV (e.g. Kilauea: Zablocki, 1976; Unzen: Hashimoto and Tanaka, 1995; Miyake-jima: Sasai et al., Aso: Hase et al., 2005). Streaming potential is the presumable SP mechanism, which is made by electric charges associated with hydrothermal upwelling (Ishido and Mizutani, 1981). Therefore, SP method is useful for the investigation of subsurface water flow.

Usu volcano is one of the most active volcano in Japan, located at the southern margin of Toya caldera, Hokkaido Island, northern part of Japan, which is constructed by basalt-basaltic andesite stratovolcano, three dacite lava domes (O-Usu, Ko-Usu, Showa-Shinzan) and many crypto domes (e.g. Soya et al., 2007). Active fumaroles are located in the summit caldera of the volcano.

Several SP surveys on Usu volcano were conducted. The first SP survey was conducted at the Toya hot spring area and discussed for flow path of the hot spring water by Yamaguchi at al. (1954). After few decades suspended, SP surveys were conducted at the summit area of the volcano in 1983, 1985, 1987, and 1994, which revealed a positive SP anomaly over +400 mV and discussed for hydrothermal system into the volcano (Nishida and Tomiya, 1987; Matsushima et al., 1990; Nishida et al., 1996). After the 2000-eruption, SP survey was conducted on the eruptive area of the volcano, which revealed a positive SP anomaly of several dozen mV and its time variation (Saba et al., 2007). The past all SP surveys were conducted in the limited area of the volcano, therefore, we conducted SP mapping survey and numerical simulations on more extensive area to clarify the hydrothermal system beneath the volcano.

2. SELF-POTENTIAL SURVEYS ON USU VOLCANO

We conducted SP measurements on the volcano in the area of 5 km (NS) by 7 km (EW) from July to December 2006 (Figure 1). The survey intervals are basically 50 m (partly 100 m to 200 m) along survey lines. We used a pair of Cu-$CuSO_4$ non-polarizable electrodes contained in ceramic pots and employed a digital multimeter with 1000 MΩ of input impedance. To assure a good contact of the electrode with ground, we inserted a piece of moisturized bentonite clay between soil and the electrodes. The survey network contains many loops so that we can evaluate the closure offsets (loop errors). The maximum closure offset of the surveys was 19.5 mV, which is small enough to discuss the SP anomalies in this study.

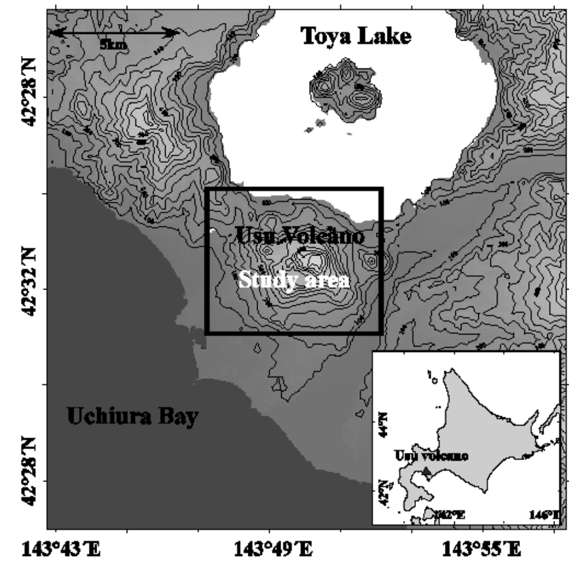

Figure 1: Location map of Usu volcano (inset) and a topographic map around the volcano. A thick square shows study area of this paper.

Figure 2 shows a compiled map of raw SP distribution. The main feature of this map shows that positive SP anomalies can be seen on lower altitudes. In the summit caldera areas, negative SP anomalies can be seen on the flank and the summit of O-Usu, Nishiyama, and Ko-Usu areas. At the flank of the southwestern part, the SP profile shows clear topographic effect (about -2.5mV/m). This profile implies dominant gravity-driven flow into the volcano, which is normally stable in time.

At the summit area of the volcano, a positive SP anomaly is located independently of elevation. This area includes many active fumaroles and the past SP surveys also observed the same scale of a positive anomaly, which implies that hydrothermal system is expected beneath the summit area.

3. NUMERICAL SIMULATION

3.1 Equation of Electrokinetic Phenomena

The fundamental equation of electrokinetic phenomena (e.g. Ishido and Mizutani, 1981) is:

$$I = -L_{ee}\nabla\phi - L_{ev}\nabla(P + \rho gz) \quad (1)$$

$$J = -L_{ve}\nabla\phi - L_{vv}\nabla(P + \rho gz) \quad (2)$$

where are $\boldsymbol{I}$: electric current density (A/m^2), $\boldsymbol{J}$: flow density of fluid (m/sec), ϕ: electric potential (V), $\boldsymbol{P}$: fluid pressure (Pa), ρ: fluid density (kg/m^3), $\boldsymbol{g}$: gravity acceleration (m/sec^2), and $\boldsymbol{z}$: elevation (m). The $\boldsymbol{L_{ab}}$ are the phenomenological coefficients. The first term on the right-hand side including $\boldsymbol{L_{ee}}$ in Eq.(1) represents Ohm's law, and the second term includeing $\boldsymbol{L_{vv}}$ in Eq. (2) represents Darcy's law. The terms with $\boldsymbol{L_{ev}}$ and $\boldsymbol{L_{ve}}$ correspond to the electrokinetic effect. According to Onsagar reciprocal relations, $\boldsymbol{L_{ev}}$ is equal to $\boldsymbol{L_{ve}}$ (de Groot and Mazur, 1962). The first term and second term of Eq.(1) represent conduction current density ($\boldsymbol{L_{cond}}$) and drag (convection) current density ($\boldsymbol{L_{drag}}$) respectively, and is as follows.

$$I = I_{cond} + I_{drag} \quad (3)$$

If electric charge conservation is comprised in (3), conduction current source can be expressed as follows:

$$\nabla \cdot I_{cond} = \nabla \cdot (-L_{ee}\nabla\phi) = -\nabla \cdot I_{drag} \quad (4)$$

Equation (4) is Poisson equation for ϕ and represents sources of conduction current which are a prerequisite for the appearance of electric potential at surface. The EKP postprocessor simulates electric potentials caused by subsurface fluid flow using a two-step procedure. First, it calculates the distribution of $\boldsymbol{L_{ee}}$, $\boldsymbol{L_{ev}}$ and $\boldsymbol{I_{drag}}$ from the fluid flow simulation results. Next, the postprocessor calculates the electric potential (ϕ) distribution by solving Eq. (4). The electrokinetic coupling coefficient $\boldsymbol{L_{ev}}$ is computed by the postprocessor using formulations based on the capillary model of Ishido and Mizutani (1981).

$$L_{ev} = L_{ve} = -\eta t^{-2}\varepsilon\varsigma / \mu$$

Where η and t are the porosity and tortuosity of the porous medium, respectively.

3.2 Parameter Setting

In the present study, the STAR and EKP postprocessor is used for the simulation. The grid is applied for 3D, which number is 66(X) x 66(Y) x 28(Z) and extends 20 km in horizontal direction (X and Y), 4.8 km in vertical direction (Z) (Figure 3). The rock unit of the simulation is divided into nine sub-regions with different rock properties (table 1). The first and second sub-regions representing sea and lake are assumed to have very high porosity (0.99). In the other sub-regions, the porosity is assumed to be 0.1. The STAR has several equation-of-state for purpose of simulations. We took "BRNGAS" which is applicable to a system of three pore components (H_2O, NaCl and air) and three pore phases (liquid, gas/vapor and solid halite precipitate) to calculate subsurface fluid flow in the volcano. To represent meteoric water recharge, a source of water is H_2O with 0.00036 mass fraction of NaCl, which is uniformly applied to the upper surface. Heating zone (the total is 500MW) is setting to the intruded magma area beneath Usu-Shinzan (Matsushima et al., 2001) (Figure 4).

4. RESULT OF SIMULATIONS

Model A shows that negative SP anomalies (approximately -1000 mV) are located at the upper part of the summit caldera. Especially, the SP profile at the summit cones of Nishiyama and O-Usu show very negative values of -1300 mV and -2400 mV, respectively (Figure 5(a)). In contrast, the SP profile at the lower part of the volcano shows relatively positive. The SP profile in the study area briefly shows topographic effect because of heatless simulation, which are corresponding to the observed SP at the southwestern part below 150 m elevation of the volcano. However, the SP profile in the summit caldera indicates approximately 1000 mV discrepancy between observed and predicted from the simulations. Model B, including heat source, shows good agreement with model A below 150 m ASL at the volcano whereas shows +400 mV of SP higher than the model A (Figure 5(b)). It is thought to be influenced by hydrothermal upwelling driven by heat source. Comparison between the model B and observed SP, there is also in good agreement with the observed SP below 150 m ASL but SP discrepancy of +400 mV is at the summit caldera. The SP profile of Model C, including low-resistivity channels, shows -600 mV at the western part of O-Usu and -400 mV at the Ginnuma crater, which is grossly the same profile of model B and is relatively larger than the SP of model A (Figure 5(c)). There are local positive SP anomalies (approximately +200 mV) at the summit of Usu-Shinzan, southeastern of O-Usu flank, and the margin of southwestern of the summit caldera, where are located on the low-resistivity channels. Model D including heat source and low-resistivity channels shows -1,650 mV and -350 mV of SP at the summit and western part of O-Usu respectively, which are the same tendency of others (Figure 5(d)). However, the model shows +750mV larger than model A, 250 mV larger than model B and C of SP, that are in the best agreement with observed SP. The SP of the model is almost the same of superimposing model B on C, which is thought that the positive SP anomaly on the summit crater is made by superimposing between low-resistivity channels effect on streaming potential of hydrothermal upwelling.

5. CONCLUDING REMARKS

In many cases positive SP anomalies on active volcanoes including restrictive and scattered local one have been thought to be caused by hydrothermal upwelling driven by heat source. The result of numerical simulations indicates that hydrothermal upwelling always made a concentric and widely SP anomaly on the surface, which is difficult to make restrictive and scattered anomaly. In contrast, a low resistivity channels stretched to the vertical direction can make a restrictive and scattered positive SP anomaly on the surface. The positive SP anomaly on the summit caldera of Usu volcano can be interpreted as caused by hydrothermal upwelling driven by the intruded conduit beneath Usu-shinzan superimposing on the effect of low-resistivity channels from the upper margin of the hydrothermal area to the surface (Figure 6).

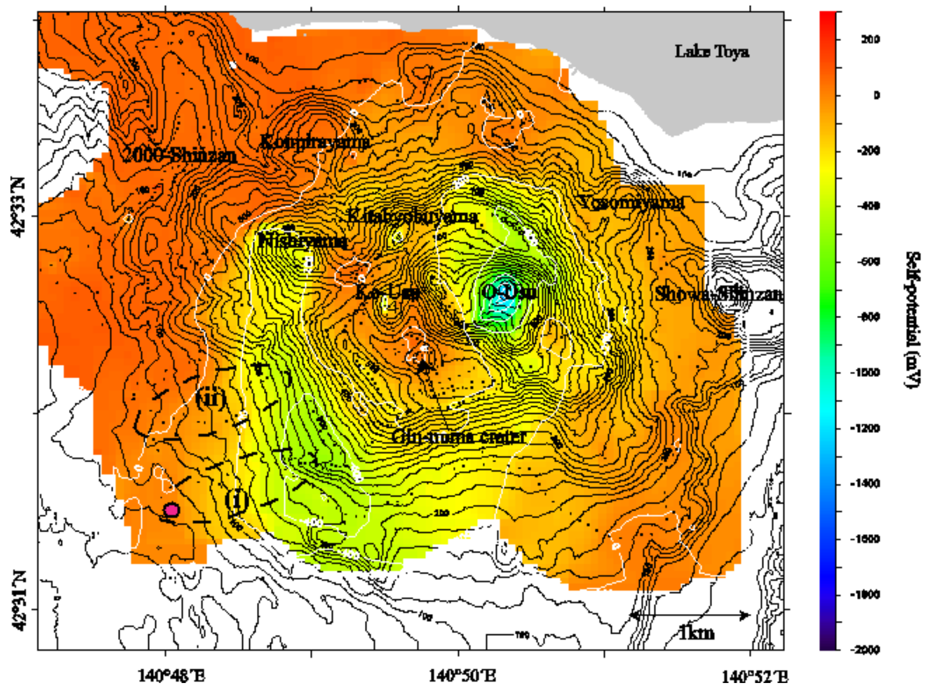

Figure 2: Raw self-potential (SP) distribution with color contours. Black dots show survey points. White and black contours indicate SP value and elevation, respectively. A circle mark located at the southwestern in the map shows the reference point.

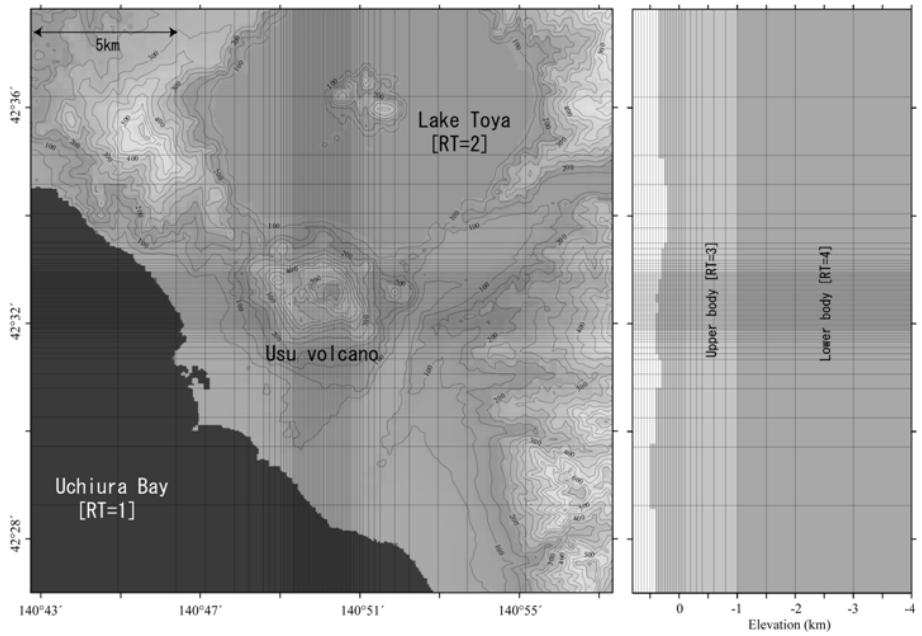

Figure 3: Simulation grid used for numerical simulations with STAR and EKP-postprocessor, plane view (left) and cross-section (right) along eastern grid. RT means rock type and the numbers indicate its category (details are shown in Table 1).

Table 1: Major parameters in STAR and EKP post-processor.

RT (rock type)	Area	Permeability[X, Y] (m^2)	Permeability[Z] (m^2)	Resistivity (Ωm)/ Mode	Coupling coefficient (V/Pa)
1	Uchiura Bay (Sea area)	1.00E-13	1.00E-13	3.3 (default) / Capillary	0.0
2	Lake Toya	1.00E-13	1.00E-13	10.0 (default) / Capillary	0.0
3	Upper body (> -1km)	5.00E-15	5.00E-15	1000.0 (default) / Capillary	-6.3E-07
4	Lower body (< 1km)	1.00E-15	1.00E-15	1000.0 (default) / Capillary	-8.7E-07
5	Hydrothermal area	1.00E-12	8.00E-13	1.0 (default) / Capillary	-2.0E-10
6	Altered low-permeable area	1.00E-16	1.00E-17	2.0 / Fixed	-2.8E-09
7	Altered low-permeable area2	5.00E-13	5.00E-17	100.0 / Fixed	-1.4E-07
8	Heat source area	1.00E-17	1.00E-17	1000.0 / Fixed	-2.1E-07
9	Upper part of the summit caldera	5.00E-14	5.00E-14	1000.0 (default) / Capillary	-1.7E-06

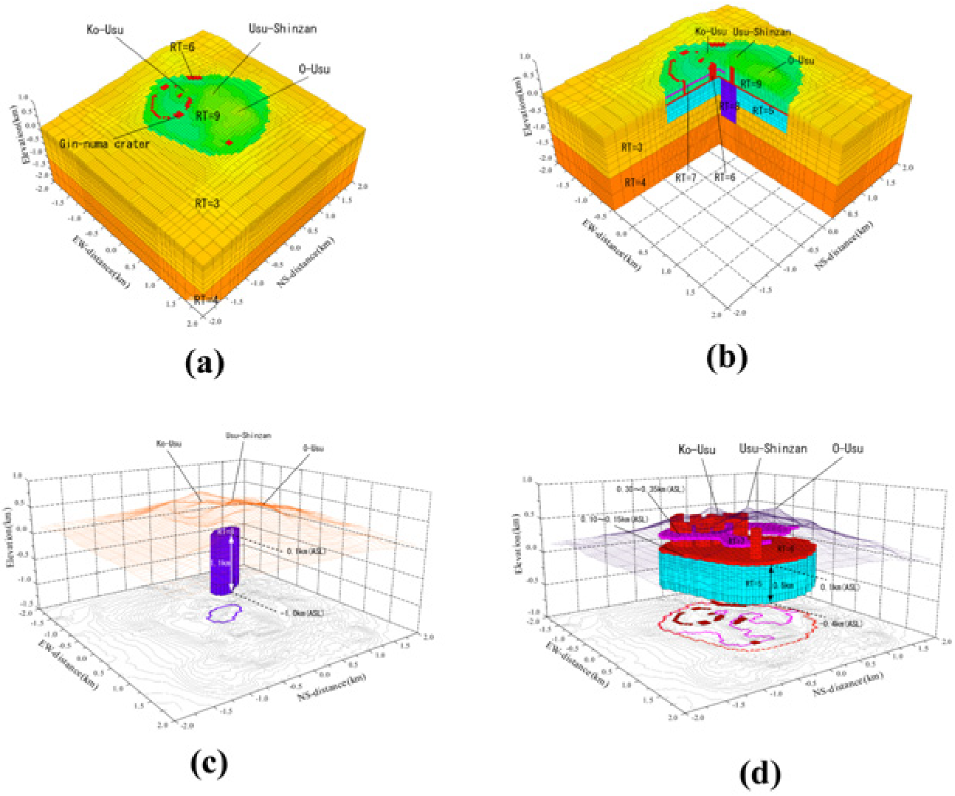

Figure 4: Simulation grid with STAR and EKP-postprocessor and the rock type locations at the central part of the Usu volcano. (a) Surface grid distribution with rock type categories. (b) Surface and sectional grid distribution with rock type categories. (c) The location of heat source grid (RT8). (d) The locations of hydrothermal grid (RT5), low permeable and resistivity grid (RT6), and surface low resistivity grid (RT7).

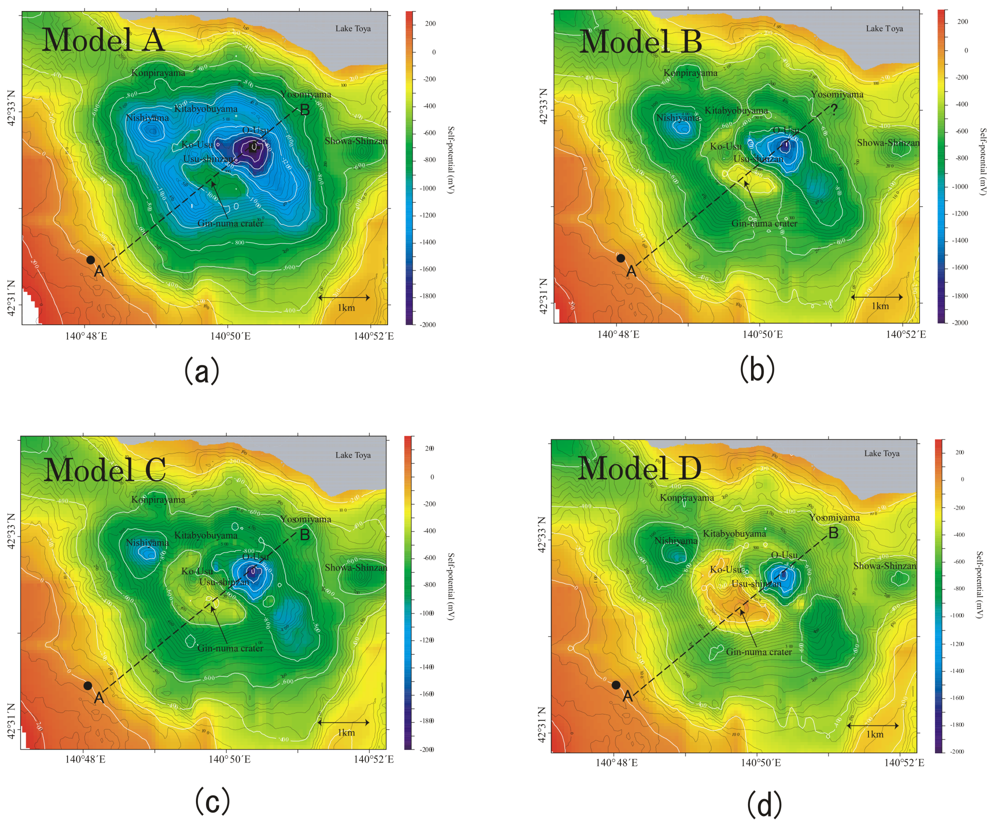

Figure 5: The results of SP simulations under the conditions of (a)without heat sources and low-resistivity channel conduits, (b)with heat sources without low-resistivity channel conduits, (c)with low-resistivity channel conduits without heat sources, and (d)with heat sources and low-resistivity channel conduits. Black dots show the reference points which are the same reference point of the observed SP in Figure 2.

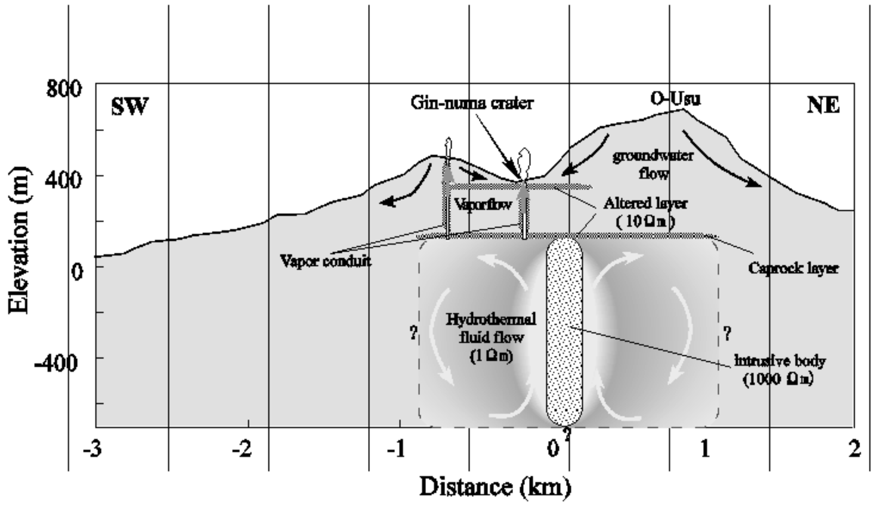

Figure 6: Schematic image of hydrothermal system beneath Usu volcano.

REFERENCES

Hase, H., Hashimoto, T., Sakanaka, S., Kanda, W. and Tanaka, Y. (2005). Hydrothermal system beneath Aso volcano as inferred from self-potential mapping and resistivity structure. *J. Volcanol. Geotherm. Res.*, 143, pp.259-277.

Hashimoto, T. and Tanaka, Y. (1995). A large self-potential anomaly on Unzen volcano, Shimabara peninsula, Kyushu island, Japan. *Geophys. Res. Lett.*, 22, pp.191-194.

Ishido, T., and Mizutani, H. (1981). Experimental and theoretical basis of electrokinetic phenomena in rock-water systems and its applications to geophysics. *J. Geophys. Res.*, 86, pp.1763-1775.

Matsushima, N., Michiwaki, M., Okazaki, N., Ichikawa, R., Takagi, A. and Nishida, Y. (1990). Self-potential studies in volcanic areas (2) – Usu, Hokkaido Komagatake and Me-akan –. *J. Fac. Sci. Hokkaido Univ. Ser. 7*, 8, pp.465-477.

Matsushima, N., Oshima, H., Ogawa, Yl, Takakura, S., Satoh, H., Utsugi, M, and Nishida, Y. (2001). Magmaprospecting in Usu volcano, Hokkaido, Japan using magnetotelluric soundings. *J. Volcanol. Geotherm. Res.*, 109, pp.263-277.

Nishida, Y. and Tomiya, H. (1987). Self-potential studies in volcanic areas (1) – Usu volcano -. *J. Fac. Sci. Hokkaido Univ. Ser. 7*, 8, pp.173-190.

Nishida, Y., Matsushima, N., Goto, A., Nakayama, Y., Oyamada, A., Utsugi, M. and Oshima, M. (1996). Self-potential studies in volcanic areas (3) – Miyake-jima, Esan and Usu-. *J. Fac. Sci. Hokkaido Univ. Ser. 7*, 10, pp.63-77.

Saba, M., Nishida, Y., Mogi, T., Takakura, S. and Matsushima, N. (2007). Development of geothermal field following the 2000 eruption of Usu volcano as revealed by ground temperature, resistivity and self-potential variations. *Annals of Geophysics*, 50, pp.79-92.

Sasai, Y., Zlotnicki, J., Nishida, Y., Yvetot, P., Morat, P., Murakami, H., Tanaka, Y., Ishikawa, Y., Koyama, S., and Sekiguchi, W. (1997). Electromagnetic monitoring of Miyake-jima volcano, Izu-Bonin arc, Japan : a preliminary report, *J. Geomagn. Geoelectr.*, 49, pp.1293-1316.

Soya, T., Katsui, Y., Niida, K. and Sakai, K. (2007). Geological map of Usu volcano (second edition). Geological Survey of Japan, AIST.

Zablocki, C. J. (1976). Mapping thermal anomalies on an active volcano by the self potential method, Kilauea, Hawaii. *Proc. 2nd U. N. Symp. On the Development and Use of Geothermal Resources*, 2, pp.1299-1309.